Journal of the Korean Ceramic Society
Vol. 55, No. 4, pp. 358–363, 2018.

https://doi.org/10.4191/kcers.2018.55.4.06

$Pr_2NiO_{4+\delta}$ for Cathode in Protonic Ceramic Fuel Cells

Hyegsoon An*,*, Dongwook Shin**,****, and Ho-Il Ji*,†**

**High-temperature Energy Materials Research Center, Korea Institute of Science and Technology, Seoul 02792, Korea*
***Department of Fuel Cells and Hydrogen Technology, Hanyang University, Seoul 04763, Korea*
****Division of Materials Science and Engineering, Hanyang University, Seoul 04763, Korea*

(Received April 13, 2018; Revised May 29, 2018; Accepted May 29, 2018)

ABSTRACT

To improve the polarization property of cathodes, which is the main factor limiting the performance of protonic ceramic fuel cells (PCFCs), K_2NiF_4-type $Pr_2NiO_{4+\delta}$, which is expected to exhibit a triple conducting property (proton, oxygen ion, and hole conductions) was applied to PCFCs and its properties were investigated. Low-temperature microwave heat-treatment was used to achieve both sufficient interface adhesion between the electrolyte and the cathode layers and suppression of the secondary phase formation due to migration of elements such as barium and cerium. Through this fabrication method, a high performance of 0.82 $W \cdot cm^{-2}$ and low ohmic resistance of 0.06 $\Omega \cdot cm^2$ were obtained in an Ni-$BaCe_{0.55}Zr_{0.3}Y_{0.15}O_{3-\delta}$ | $BaCe_{0.55}Zr_{0.3}Y_{0.15}O_{3-\delta}$ | $Pr_2NiO_{4+\delta}$ single cell at 650°C. This result verifies that the $K_2NiF_{4+\delta}$-type cathode shows good chemical compatibility which, in turn, will make it a potent candidate as a PCFC cathode.

Key words : Proton ceramic fuel cells, Cathode, Microwave sintering

1. Introduction

Proton ceramic fuel cells (PCFCs) are an intermediate temperature-solid oxide fuel cells (IT-SOFCs) with high performance, fuel flexibility, and predicted enhancements of reliability and durability through low temperature operation.[1] Especially, the conduction phenomenon of protons, which occurs through the hydration reaction under a humid environment, distinguishes PCFCs from other IT-SOFCs, but this phenomenon induces differences in the operation mechanism, making the selection of the cathode material difficult. For example, the cathode material of PCFC has simultaneously to be chemically stable for the operation conditions (intermediate temperature humid environment) and to exhibit high electrochemical properties. Also, the use of triple conducting oxide (TCO) cathode materials that satisfy the proton, oxygen ion, and hole conducting properties is predicted to maximize the electrode reaction area and, according to the operating principle, result in high electrochemical properties.[2,3] Recently, electrochemical impedance spectroscopy (EIS) and thermogravimetric analysis (TG) results for lanthanide nickelate ($Ln_2NiO_{4+\delta}$, Ln = La, Pr) showed that $Pr_2NiO_{4+\delta}$ is a potent TCO material.[2,4] Moreover, whereas the typical proton conductive perovskite-type electrolyte materials possess oxygen vacancies, lanthanide nickelate has interstitial oxygen ion sites within the rock salt layer, and in turn, the outstanding chemical stability in humid environments and the high electrode properties (oxygen ion diffusivity (8×10^{-8} cm^2S^{-1} at 750°C); surface exchange coefficient (6×10^{-6} cmS^{-1} at 750°C) have been reported.[5,6] It implies the applicability of lanthanide nickelate as a PCFC cathode.

Therefore, to assess the electrochemical properties in this study, the $Pr_2NiO_{4+\delta}$ material predicted to exhibit the TCO property was selected as the PCFC cathode. Secondary phase formation from the reaction between the electrolyte and cathode was observed as reported by various studies and a single cell was fabricated using microwave heat treatment in order to minimize the secondary phase formation. Cost-effective process design of low temperature and short duration is possible using the microwave heat treatment process, which heats the specimen through interaction with microwaves, in comparison to conventional heat treatment method. Furthermore, due to the process characteristics that accelerate diffusion process and extremely suppress crystal grain growth, the process is appropriate for heat treatment of a cathode film for which a porous microstructure is preferred for low polarization resistance and to overcome the electrolyte/anode differential sintering behavior to induce a high degree of interfacial adhesion.

2. Experimental Procedure

The $BaCe_{0.55}Zr_{0.3}Y_{0.15}O_{3-\delta}$ (BCZY3), $Pr_2NiO_{4+\delta}$ (PrN) powder was prepared using the 2-step solid state reaction method. First, adequate amounts of $BaCO_3$ (Cerac, USA, 99.99%), CeO_2 (High Purity Chemical, Japan 99.99%), ZrO_2 (Tosoh, Japan), and Y_2O_3 (High Purity Chemical, Japan 99.99%) were dried in a 200°C oven for 24 h and ethanol was added for ball-milling, carried out for 24 h. The obtained powder

†Corresponding author : Ho-Il Ji
E-mail : hiji@kist.re.kr
Tel : +82-2-958-5521 Fax : +82-2-958-5529

underwent calcination for 10 h at 1300°C and 1400°C, followed by ball-milling for 48 h.[7] Next, Pr_6O_{11} (Aldrich, USA, 99.9%) and NiO (Sumitomo, Japan) were used as starting materials for the synthesis of PrN. The prepared powder underwent ball-milling for 24 h with ethanol followed by calcination for 10 h at 1000°C and 1100°C and ball-milling for 24 h with ethanol. The crystalline structure of the produced powder was investigated using X-ray diffraction (XRD) under the conditions of 20° - 80° and 1°/min using a D max 2500/PC (Rigaku, Japan).

In order to evaluate the high temperature chemical compatibility of the electrolyte and cathode powders, ball-milling with ethanol was conducted for equal volumes of the BCZY3 and PrN powders for 24 h, followed by drying. Uniaxial pressing at 100 MPa was performed to produce 10phi sized pellets. The produced samples were then heat treated for 2 h at 800°C - 1200°C and the crystalline structure changes were observed through XRD analysis.

The anode-electrolyte support was fabricated using the conventional ceramic process.[7] For the manufacturing of the anode substrate, BCZY3 and NiO (Sumitomo, Japan) powders at weight ratio of 45 : 55 were mixed with ethanol and polymer additives to induce granulation via the spray drying method. PMMA (poly methyl methacrylate) at 30% volume ratio was added to produce pores for the anode. 100 MPa uniaxial pressing was conducted for the produced granules to prepare 8 × 8 cm^2 substrates. For the formation of the anode functional layer and electrolyte layer, the BCZY3, NiO mixture powder and BCZY3 powder were each mixed with α-terpinol (Kanto Chemical, Japan) and polymer additives. The obtained paste was screen printed on the prepared anode substrate and then co-fired for 4 h at 1350°C.

The cathode layer was prepared using a microwave oven. The synthesized PrN powder was mixed with α-terpinol and polymer additives and screen printed on the anode-electrolyte substrate over an area of 1 × 1 cm^2. Heat treatment was performed at 800°C, 900°C, and 950°C for 1 minute each using a microwave oven (UMF-04, UNICERA, Korea).

A lab-made station was used to measure the electrochemical performance of the cell. Humidified H_2 and dry air were supplied at 200 sccm each to the anode and cathode. An electrochemical analyzer (IviumStat, Netherlands) was used to assess the open circuit voltage (OCV), current-voltage curves (IV), and electrochemical impedance spectra (EIS) characteristics in the temperature range of 500°C - 650°C.

After the evaluation, the cell microstructure was investigated using a scanning electron microscope (SEM, Inspect F50, FEI).

3. Results and Discussion

The XRD results for the PrN powder according to the calcination temperature are shown in Fig. 1. As the heat treatment temperature increased from 1000°C to 1100°C, the XRD results showed that the unreacted phases, which were

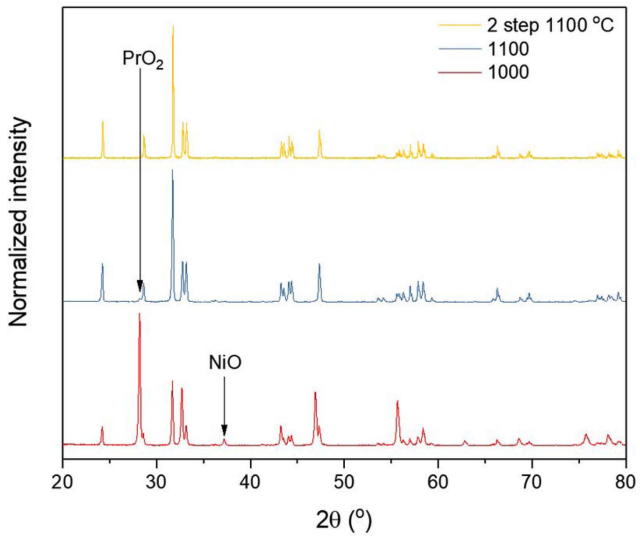

Fig. 1. X-ray diffraction patterns of $Pr_2NiO_{4+\delta}$ calcined at various temperatures.

PrO_2 at 28.18° (PDF#04-004-1605) and NiO at 37.2° and 62.83° (PDF#04-006-6160), disappeared. Afterwards, calcination was carried out again under the same conditions to remove the small amount of PrO_2 unreacted phase remaining in the 1100°C-calcined powder. This was done because, when additionally increasing the PrN calcination temperature, reduction of the cathode activation is inevitable due to the reaction with the Al_2O_3 crucible and high temperature grain growth. Meanwhile, the XRD results showed that the calcined PrN has an orthorhombic (Fmmm) crystalline structure, which is in agreement with the literature.[2,8-10] PrN with a K_2NiF_4-type crystalline structure composed of the $PrNiO_{3-\delta}$ perovskite layer and PrO rock salt layer was reported to show phase transition from orthorhombic (Fmmm) to tetragonal (I4/mmm) structure as the numerous oxygen interstitial sites within the rock salt layer are filled, and the maximum value of the interstitial oxygen (δ) was reported to be 0.22.[11] The XRD and Rietveld refinement analysis results of the synthesized BCZY3 powder showed a single phase rhombohedral (R3-c) crystalline structure and were in agreement with the literature ($BaCe_{0.55}Zr_{0.3}Y_{0.15}O_{3-\delta}$, PDF#04-018-2314).[12] Table 1 shows the lattice constant and lattice volume, determined using an XRD analysis program (JADE 9.0, Japan).

For the formation of the cathode layer, high temperature chemical compatibility with the electrolyte needs to be considered. In particular, it has been reported that the Ln contained in the lanthanide nickelate ($Ln_2NiO_{4+\delta}$; Ln = La, Pr) type cathode material consumes Zr and Ce within the electrolyte to form a reaction layer and severely reduce the cell performance.[4,13,14] When yttrium-doped $BaCeO_3$ (BCY) and PrN are used as the electrolyte and cathode materials, respectively, it was reported that a $(PrCe)O_2$ interfacial reaction layer is formed; Pr and Ce can exist in various ratios, exhibiting oxygen ion conduction characteristics.[15]

Table 1. Rietveld Refinement Results of Calcined $BaCe_{0.55}Zr_{0.3}Y_{0.15}O_{3-\delta}$ and $Pr_2NiO_{4+\delta}$

Composition	Crystal structure	a (Å)	b (Å)	c (Å)	Cell Vol (Å^3)
$BaCe_{0.55}Zr_{0.3}Y_{0.15}O_{3-\delta}$ (PDF#98-018-1963)	Rhombohedral (R3-c)	6.1393		14.9615	488.3638
$Pr_2NiO_{4+\delta}$ (PDF#01-086-0870)	Orthorhombic (Fmmm)	5.3923	5.4561	12.4469	366.2

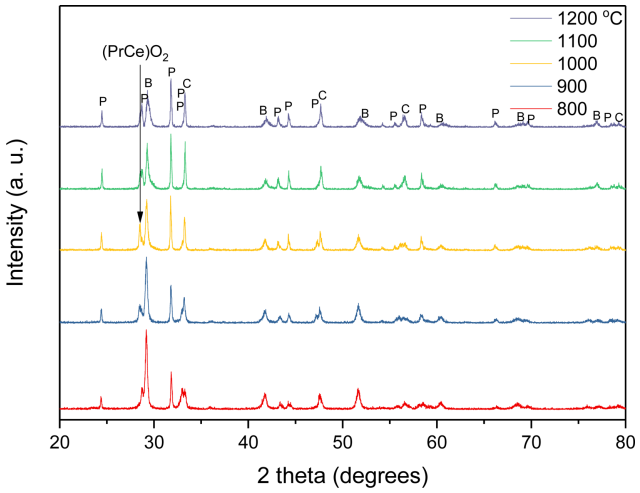

Fig. 2. Chemical compatibility between BCZY3 and PrN (BCZY: B, PrN: P and $(PrCe)O_2$: C).

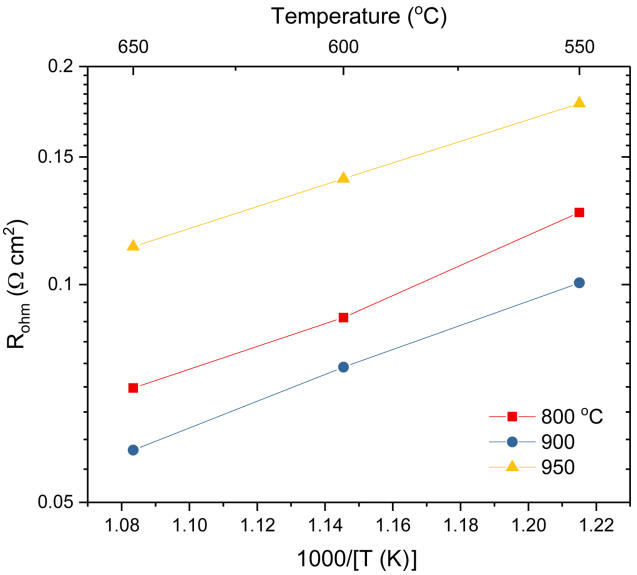

Fig. 3. Arrhenius plot of area-specific ohmic resistance from impedance spectra of Ni-BCZY3 | BCZY3 | PrN cells in which cathodes were sintered at 800°C, 900°C, and 950°C, respectively.

However, proton conductivity has not been reported. Thus, in order to determine the heat treatment temperature at which there is no reaction between the electrolyte and cathode, a high temperature compatibility test was conducted. Fig. 2 shows the XRD results after heat treatment at various temperatures, performed to examine the high temperature chemical compatibility between the BCZY3 electrolyte and PrN cathode. A $(PrCe)O_2$ fluorite-type (PDF# 04-006-3411) reaction phase at around 28.53° was observed for the heat treatment condition of above 900°C. As the heat treatment temperature increased, the peak magnitude increased due to the reaction phase and it was found that the peak corresponding to the PrN phase shifted to high angle. It was reported that Ba forms $Pr_{2-x}Ba_xNiO_{4+\delta}$ phase via reaction with $Pr_2NiO_{4+\delta}$, and the cell volume decreased ($x < 0.3$) as the amount of substituted Ba increased.[16] Therefore, the PrN phase peak shift to the high angle as temperature increases implies the formation of $Pr_{2-x}Ba_xNiO_{4+\delta}$ phase, and this signifies that cation inter-diffusion between the BCZY3 electrolyte and PrN occurs. As a result, the reaction between the electrolyte and cathode was observed for temperatures above 900°C.

Electrochemical properties of a single cell according to the temperature of microwave heat treatment for the PrN cathode material were measured by electrochemical impedance spectroscopy (EIS) for each temperature. Fig. 3 shows the ohmic resistance as a function of heat treatment temperature for the cathode. The ohmic resistance was obtained from the high frequency intercept of impedance spectra. From the fact that the secondary phase that was formed due to the reaction between the electrolyte and the cathode at temperatures higher than 900°C in XRD results, an increase in the ohmic resistance for the 950°C heat treatment case, compared to the 900°C case, suggests that the formed secondary phase increases the single cell ohmic resistance. On the other hand, the resistance increase for the 800°C heat treatment case, for which no interfacial reaction was observed, led to the conjecture that insufficient interfacial adhesion caused the ohmic resistance increase. Based on this results, the electrochemical properties of the optimized single cell, which was heat-treated at 900°C, were analyzed. Fig. 4(a) shows a Nyquist plots according to the temperature for the single cell heat treated at 900°C. The single cell polarization resistance was obtained from the difference between the total resistance and the ohmic resistance. For temperatures of 650, 600, 550, and 500°C, the ohmic resistances were 0.06, 0.08, 0.1, and 0.14 Ωcm^2, respectively, and the polarization resistances were 0.13, 0.28, 0.68, and 1.7 Ωcm^2, respectively. The activation energy, determined from the single cell ohmic resistance, was 0.42 eV, which shows that ionic conduction within the electrolyte was all through protons.[17,18] Fig. 4(b) shows the voltage and power density evaluation results for the single cell according to the current. The peak power densities (PPD) for tem-

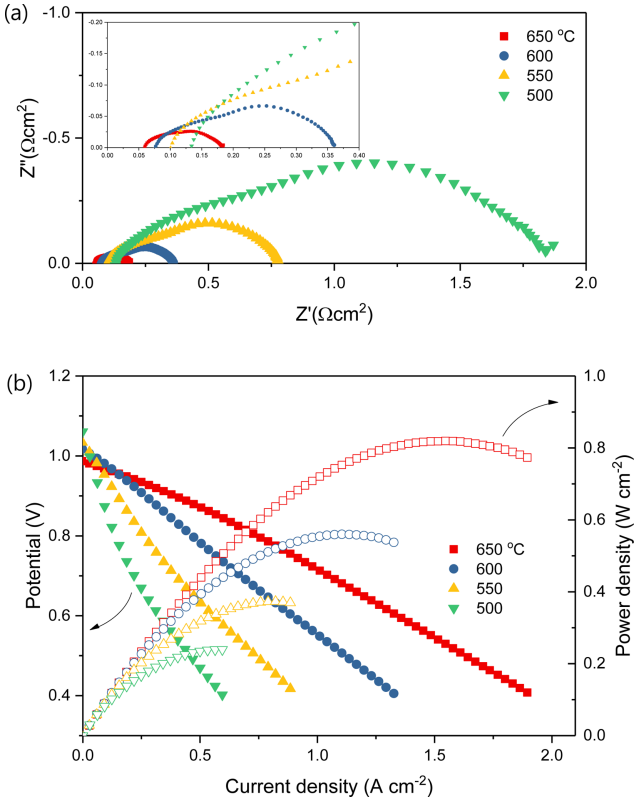

Fig. 4. (a) Electrochemical impedance spectra and (b) potential and power density curves as a function of current density in temperature range of 650°C - 500°C for Ni-BCZY3 | BCZY | PrN cell in which PrN was sintered at 900°C.

peratures of 650, 600, 550, and 500°C were 0.82, 0.56, 0.37, and 0.24 W·cm^{-2}, respectively. These values are the highest among previously reported PrN-based PCFC studies to the best of our knowledge. The 1200°C heat treatment case of PrN for the BCY electrolyte was reported to have power density of 0.13 W·cm^{-2} at 650°C, while the 1100°C heat treatment case for the BCZY electrolyte had a power density of 0.16 W·cm^{-2}. This difference clearly shows the effect of electrochemical property degradation due to electrolyte and cathode interfacial reaction on the PCFC power density performance. In detail, the previous single cell ohmic resistance results of 1.36 Ωcm^2 for 40 μm BCY and 0.696 Ωcm^2 for 5 mm BCZY at 650°C show significant differences with this result of 0.06 Ωcm^2 for 5 μm BCZY in this study, and these reported values are very large compared to the expected values based on the chemical composition of the bulk electrolyte. In summary, minimizing the degradation in properties that arises from the cathode heat treatment process was achieved by the low-temperature microwave process, and it resulted in appropriate levels of electrode properties for PrN as a PCFC cathode material.[14,19] The single cell open circuit voltages (OCV) were 0.99, 1.02, 1.03, and 1.06 V for temperatures of 650, 600, 550, and 500°C, respectively, which were similar to the results of studies that used BCZY electrolyte.[19]

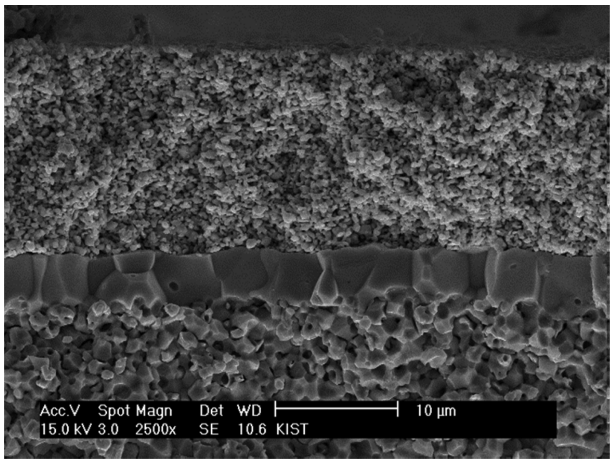

Fig. 5. Cross-sectional microstructure image of Ni-BCZY3 | BCZY3 | PrN single cell after test.

After the cell measurements, the microstructure and crystalline structure were investigated for post analysis. Fig. 5 shows the microstructure of the single cell after the electrochemical analysis. The PrN cathode layer that was fabricated by microwave process showed sufficient interfacial adhesion even after the electrochemical measurements; no delamination was observed. This result showed that sufficient interfacial adhesion between the electrolyte and cathode was achieved by microwave heat treatment and this was thought to be due to the similar thermal coefficients of expansion between PrN and the BCZY electrolyte (thermal expansion coefficient α (K^{-1}) = 10.8×10^6 for BCZY, 13.6×10^6 for PrN).[5,10,20] If the $(PrCe)O_2$ reaction layer is formed on the electrolyte-cathode interface, it is difficult to maintain the interface due to the rapidly increasing thermal expansion behavior at temperatures above 400°C (thermal expansion coefficient α (K^{-1}) = 26×10^{-6} for $(PrCe)O_2$).

Moreover, the XRD results for the surface of the cathode shown in Figs. 1 and 6 indicate that secondary phase formation due to i) the reaction between the BCZY3 electrolyte and the PrN cathode material and ii) the PrO phase formation due to the decomposition of PrN[11] ($Pr_2NiO_{4+\delta} \rightarrow Pr_4Ni_3O_9 + PrO_{1.75}$) do not occur. In detail, the PrO peak existing at 28.18° for temperatures of 1000 and 1100°C, shown in the Fig. 1 XRD results, was not present after synthesis (Fig. 1 1100°C 2step) and after the measurement (Fig. 6). An interesting point was that a merging of the split peak formed due to the orthorhombic symmetricity in the PrN XRD pattern was observed. For example, it was observed that the (200) and (020) planes at 32.799° and 33.198° in the orthorhombic (Fmmm) crystalline structure merged into the (200) plane (2θ = 32.846°) of the tetragonal ($I4_2/ncm$) crystalline structure, so that the peak intensity almost doubled. The cause of this phase transition phenomenon was thought to be either the filling of the oxygen interstitial sites in the rock salt layer within the PrN crystalline structure due to annealing during the single cell measurement or the formation of $(PrBa)_2NiO_{4+\delta}$ phase with high crystallinity as the Pr

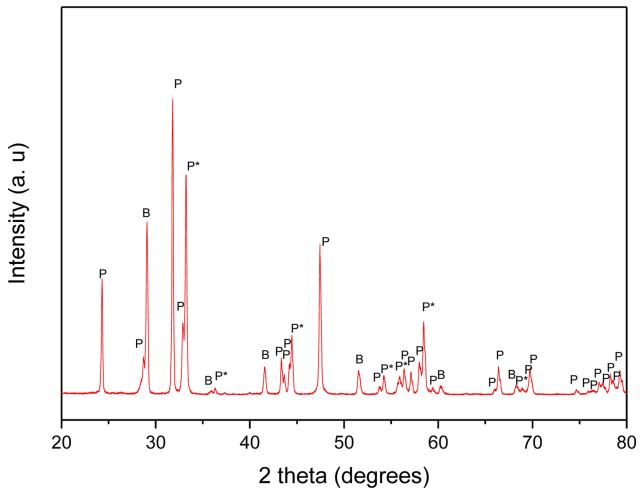

Fig. 6. X-ray diffraction pattern of PrN cathode surface in Ni-BCZY3 | BCZY3 | PrN single cell after test.

(1.179 Å) with a small ionic radius is substituted with Ba (1.47 Å). Comparison of the XRD patterns of the two reported crystalline structures (Over-stoichiometric PrN (PDF#01-087-1681), substituted PrN (PDF#01-086-0872)) showed that the intensity ratios of the two XRD peaks at about 43° were similar to the former case. Therefore, it was predicted that there would be a phase transition phenomenon from orthorhombic to tetragonal due to interstitial oxygen; this result is in agreement with the reports of increasing interstitial oxygen for intermediate temperatures.[2)] In Fig. 6, the marking P* indicates the point of XRD intensity increase according to this PrN crystallinity recovery. The fact that delamination was not observed even when the PrN cell volume increased due to the increase of interstitial oxygen (δ) signifies that the microwave-assisted low temperature cathode heat treatment process resulted in the sufficient interfacial adhesion.

4. Conclusions

$Pr_2NiO_{4+\delta}$ material with high chemical stability and excellent electrochemical properties was used as a PCFC cathode. A cathode fabrication on BCZY3 electrolyte using low-temperature microwave process was able to minimize the secondary phase formation due to the high temperature chemical reaction between the BCZY3 electrolyte and PrN cathode material. As a result, the PrN cathode that underwent microwave heat treatment at 900°C exhibited low interfacial resistance and outstanding electrochemical performance (0.06 Ω·cm^2 and 0.82 W·cm^{-2} at 650°C). This result verified that lanthanide nickelate is applicable as the PCFC cathode material.

Acknowledgments

This work was conducted as part of the National Research Foundation of Korea (NRF) grant funded by the Ministry of Science, ICT & Future Planning (2017M1A2A2044982) and as part of the Manpower Development Program for Energy supported by the Ministry of Knowledge and Economy (MKE).

REFERENCES

1. E. D. Wachsman and K. T. Lee, "Lowering the Temperature of Solid Oxide Fuel Cells," *Science*, **334** [6058] 935-39 (2011).
2. A. Grimaud, F. Mauby, J. M. Bassat, S. Fourcade, M. Marrony, and J. C. Grenier, "Hydration and Transport Properties of the $Pr_{2-x}Sr_xNiO_{4+\delta}$ Compounds as H+-SOFC Cathodes," *J. Mater. Chem.*, **22** [31] 16017 (2012).
3. R. R. Peng, T. Z. Wu, W. Liu, X. Q. Liu, and G. Y. Meng, "Cathode Processes and Materials for Solid Oxide Fuel Cells with Proton Conductors as Electrolytes," *J. Mater. Chem.*, **20** [30] 6218-25 (2010).
4. P. Batocchi, F. Mauvy, S. Fourcade, and M. Parco, "Electrical and Electrochemical Properties of Architectured Electrodes based on Perovskite and A_2MO_4-Type Oxides for Protonic Ceramic Fuel Cell," *Electrochim. Acta,* **145** 1-10 (2014).
5. E. Boehm, J. M. Bassat, P. Dordor, F. Mauvy, J. C. Grenier, and P. Stevens, "Oxygen Diffusion and Transport Properties in Non-Stoichiometric LnNiO Oxides," *Solid State Ionics*, **176** [37-38] 2717-25 (2005).
6. A. Grimaud, F. Mauvy, J. M. Bassat, S. Fourcade, L. Rocheron, M. Marrony, and J. C. Grenier, "Hydration Properties and Rate Determining Steps of the Oxygen Reduction Reaction of Perovskite-Related Oxides as H^+-SOFC Cathodes," *J. Electrochem. Soc.*, **159** [6] B683-94 (2012).
7. H. An, D. Shin, S. Choi, J. Lee, J. Son, B. Kim, H. Je, H. Lee, and K. Yoon, "$BaCeO_3$-$BaZrO_3$ Solid Solution (BCZY) as a High Performance Electrolyte of Protonic Ceramic Fuel Cells (PCFCs)," *J. Korean Ceram. Soc.*, **51** [4] 271-77 (2014).
8. V. A. Sadykov, E. M. Sadovskaya, E. Y. Pikalova, A. A. Kolchugin, E. A. Filonova, S. M. Pikalov, N. F. Eremeev, A. V. Ishchenko, A. I. Lukashevich, and J. M. Bassat, "Transport Features in Layered Nickelates: Correlation between Structure, Oxygen Diffusion, Electrical and Electrochemical Properties," *Ionics*, **24** [4] 1181-93 (2018).
9. E. Dogdibegovic, Q. S. Cai, N. S. Alabri, W. B. Guan, and X. D. Zhou, "Activity and Stability of $(Pr_{1-x}Nd_x)_2NiO_4$ as Cathodes for Solid Oxide Fuel Cells III. Crystal Structure, Electrical Properties, and Microstructural Analysis," *J. Electrochem. Soc.,* **164** [2] F99-106 (2017).
10. X.-D. Zhou, J. W. Templeton, Z. Nie, H. Chen, J. W. Stevenson, and L. R. Pederson, "Electrochemical Performance and Stability of the Cathode for Solid Oxide Fuel Cells: V. High Performance and Stable Pr_2NiO_4 as the Cathode for Solid Oxide Fuel Cells," *Electrochim. Acta*, **71** 44-9 (2012).
11. P. Odier, C. Allancon, and J. M. Bassat, "Oxygen Exchange in $Pr_2NiO_{4+\delta}$ at High Temperature and Direct Formation of $Pr_4Ni_3O_{10-x}$," *J. Solid State Chem.*, **153** [2] 381-85 (2000).

12. L. Malavasi, C. Tealdi, C. Ritter, V. Pomjakushin, F. Gozzo, and Y. Diaz-Fernandez, "Combined Neutron and Synchrotron X-ray Diffraction Investigation of the $BaCe_{0.85-x}Zr_xY_{0.15}O_{3-\delta}$ ($0.1 \leq x \leq 0.4$) Proton Conductors," *Chem. Mater.*, **23** [5] 1323-30 (2011).
13. M. A. Laguna-Bercero, H. Monzon, A. Larrea, and V. M. Oreara, "Improved Stability of Reversible Solid Oxide Cells with a Nickelate-Based Oxygen Electrode," *J. Mater. Chem. A*, **4** [4] 1446-53 (2016).
14. G. Taillades, J. Dailly, M. Taillades-Jacquin, F. Mauvy, A. Essouhmi, M. Marrony, C. Lalanne, S. Fourcade, D. J. Jones, J. C. Grenier, and J. Roziere, "Intermediate Temperature Anode-Supported Fuel Cell Based on $BaCe_{0.9}Y_{0.1}O_3$ Electrolyte with Novel Pr_2NiO_4 Cathode," *Fuel Cells*, **10** [1] 166-73 (2010).
15. R. Chiba, H. Taguchi, T. komatsu, H. Orui, K. Nozawa, and H. Arai, "High Temperature Properties of $Ce_{1-x}Pr_xO_{2-\delta}$ as an Active Layer Material for SOFC Cathodes," *Solid State Ionics,* **197** [1] 42-8 (2011).
16. Y. Chung, Y. Kwon, and S. Byeon, "Synthesis, Structural and Electrical Characterizations of $Pr_{2-x}Ba_xNiO_{4\pm\delta}$," *Bull. Korean Chem. Soc.*, **16** [2] 120-25 (1995).
17. H. Iwahara, "Oxide-Ionic and Protonic Conductors Based on Perovskite-Type Oxides and Their Possible Applications," *Solid State Ionics*, **52** [1-3] 99-104 (1992).
18. K. D. Kreuer, "Proton-Conducting Oxides," *Annu. Rev. Mater. Res.,* **33** 333-59 (2003).
19. N. Nasani, D. Ramasamy, S. Mikhalev, A. V. Kovalevsky, and D. P. Fagg, "Fabrication and Electrochemical Performance of a Stable, Anode Supported Thin $BaCe_{0.4}Zr_{0.4}Y_{0.2}O_{3-\delta}$ Electrolyte Protonic Ceramic Fuel Cell," *J. Power Sources,* **278** 582-89 (2015).
20. Y. G. Lyagaeva, D. A. Medvedev, A. K. Demin, P. Tsiakaras, and O. G. Reznitskikh, "Thermal Expansion of Materials in the Barium Cerate-Zirconate System," *Phys. Solid State,* **57** [2] 285-89 (2015).